

Extracellular Vesicles Derived From Human Adipose-Derived Stem Cell Prevent the Formation of Hypertrophic Scar in a Rabbit Model

Yuan-zheng Zhu, MD, Xuan Hu, MD, Jing Zhang, MD, Zhao-hui Wang, MD,
Shu Wu, MD, and Yang-yan Yi, MD

Background: Preventing scar formation during wound healing has important clinical implications. Numerous studies have indicated that adipose-derived stem cell culture mediums, which are rich in cytokines and extracellular vesicles (EVs), regulate matrix remodeling and prevent scar formation after wound healing. Therefore, using a rabbit scar model, we tried to demonstrate which factor in adipose-derived stem cell culture mediums plays a major role in preventing scar formation (EVs or cytokines), as well as revealing the underlying mechanism.

Methods: Human adipose-derived stem cells (hASCs) were isolated from the subcutaneous adipose tissue of a healthy female donor. The surface CD markers of third-passage hASCs were analyzed by flow cytometry. The adipogenic differentiation capacity of the hASCs was detected using Oil O staining. A cultured medium of third- to five-passage hASCs was collected for EV and EV-free medium isolations. Extracellular vesicles were characterized using transmission electron microscopy, NanoSight, and the Western blotting for surface markers CD63, TSG101, and Alix. The EV-free medium was characterized by Western blotting for vascular endothelial growth factor A (VEGFA), platelet derived growth factor B (PDGFB), and transforming growth factor β 1 (TGF β 1). Eight-millimeter-diameter wounds were created on the ventral side of both ears of 16 New Zealand rabbits. A total of 0.1 mL of the human adipose-derived stem cell-extracellular vesicle (hASC-EV) or EV-free medium was locally injected into wounds made on the right ears during wound healing. Meanwhile, equal amounts of phosphate buffer saline were injected into the left ears as a control. Biopsies of the wounded skin and surrounding tissue were excised on postoperative day 28 and subjected to hematoxylin and eosin (H&E), Masson, and α -SMA immunofluorescence staining. The protein expression of α -SMA and collagen I in both scar tissues and the normal skin were evaluated via Western blotting.

Results: The hASCs expressed high levels of 49d, CD90, CD105, and CD73 but did not express CD34 or CD45. The hASCs differentiated into adipocytes under an adipogenic induction medium. Under transmission electron microscopy, the hASC-EVs were circular, bilayer membrane vesicles and approximately 95% of the particles were between 50 and 200 nm in size. The hASC-EVs expressed the same surface markers as EVs, including CD63, TSG101, and Alix and displayed little expression of VEGFA, PDGFB, and TGF β 1. The EV-free

medium had a high expression of VEGFA, PDGFB, and TGF β 1 but displayed no expression of CD63, TSG101, and Alix. In vivo, the hASC-EV treatment prevented the formation of hypertrophic scars on postoperative day 28 and suppressed collagen deposition and myofibroblast aggregation. However, the EV-free medium did not prevent the formation of hypertrophic scars on the same time point and had little effect on collagen deposition and myofibroblast aggregation when compared with the control group.

Conclusions: Our study suggests that hASCs are associated with preventive scar formation therapy because of paracrine EVs rather than cytokines. A local injection of hASC-EVs during wound healing efficiently prevented hypertrophic scar formation, which may have a clinically beneficial antiscarring effect.

Key Words: hypertrophic scar, adipose-derived stem cell, extracellular vesicle, transforming growth factor β

(*Ann Plast Surg* 2020;84: 602–607)

Dermal scars are the result of wound healing and remodeling.¹ Myofibroblast transdifferentiation with increased expression of α -smooth muscle actin (α -SMA) appears during the contraction stage of wound healing to reduce the surface area and facilitate reepithelialization.^{2–4} However, distortions in this procedure or other pathological conditions can lead to the recruitment and excessive activation of myofibroblasts that lead to the formation of hypertrophic or even keloid scars.^{3,4}

In the case of wound healing, mesenchymal stem cells (MSCs) attenuate tissue damage, inhibit fibrotic remodeling, promote angiogenesis, stimulate endogenous stem cell recruitment and proliferation, and reduce immune responses.^{5,6} However, previous studies have demonstrated that MSCs mainly exert benefits on wound healing via paracrine cytokines, and few become permanently engrafted within the tissue.^{7–10} With an abundant supply of adipose tissue and its relative ease of isolation, the culture medium (CM) of adipose-derived stem cells (ASCs) has been used in the prevention of fibrosis.^{11,12}

Extracellular vesicles (EVs) have been identified as a kind of paracrine factor enriched in CM. Previous studies have implicated that MSC-derived EVs have beneficial functions on the different stages of wound healing, including reducing inflammation, promoting angiogenesis, and regulating matrix remodeling.^{13–15} In addition, diverse fibrotic diseases can also be prevented with EV therapy.^{16–18} Therefore, the aim of this study was to demonstrate which factor of the ASC-CM plays a major role in preventing scar formation (EVs or free cytokines). To simulate the hypertrophic scars of human beings, a scar model on rabbit ears was employed.

MATERIALS AND METHODS

The Isolation and Identification of Human Adipose-Derived Stem Cells

For isolation of the human adipose-derived stem cells (hASCs), the following protocols were performed in accordance with the Declaration of Helsinki and approved by the Ethics Committee of the Second Affiliated Hospital of Nanchang University. Human subcutaneous

Received October 20, 2019, and accepted for publication, after revision February 3, 2020.

From the Department of Plastic Surgery, The Second Affiliated Hospital of Nanchang University, Jiangxi, P.R. China.

Y.-z.Z. and X.H. are co-first authors who made an equal contribution to the article.

Conflicts of interest and sources of funding: This work was supported by grants from the National Natural Science Foundation of China (81660326), Natural Science Foundation of Jiangxi Province (20171ACB20037), Youth Natural Science Foundation of Jiangxi Province (20192BAB215028), and Youth Science Foundation of the Second Affiliated Hospital of Nanchang University (2019YNQN12021). The authors declare no conflicts of interest.

Reprints: Yang-yan Yi, MD, Department of Plastic Surgery, The Second Affiliated Hospital of Nanchang University, 1 Minde Rd, Nanchang, Jiangxi, 330006, P.R. China. E-mail: yyy0218@126.com.

Copyright © 2020 The Author(s). Published by Wolters Kluwer Health, Inc. This is an open-access article distributed under the terms of the Creative Commons Attribution-Non Commercial-No Derivatives License 4.0 (CCBY-NC-ND), where it is permissible to download and share the work provided it is properly cited. The work cannot be changed in any way or used commercially without permission from the journal.

ISSN: 0148-7043/20/8405-0602

DOI: 10.1097/SAP.0000000000002357

adipose tissue was obtained from a healthy female donor, aged 22 years, who had undergone an abdominal liposuction bariatric procedure; informed consent was obtained. Immediately after the liposuction procedure, the harvested lipoaspirates were centrifuged at 1200g for 3 minutes for purification. After centrifugation, the top oil layer and the bottom fluid layer were removed. The middle layer, which contains the purified lipoaspirate, was used in subsequent experiments. The entire harvesting procedure was performed at 25°C. Ten milliliters of purified lipoaspirate was digested with an equal volume of 0.2% type I collagenase (Sigma, Silicon Valley, CA) in a constant temperature water bath shaker at 37°C for about 1 hour and filtrated by a 200- μ m metal mesh. After filtration, the residues were centrifuged at 1200g for 3 minutes, and the supernatant was discarded. Precipitates were resuspended in a CM and cultured at 37°C in the presence of 5% CO₂. The medium was first changed after 48 hours and every 24 hours afterwards. The cells were passaged after reaching 90% confluency. Third-generation cells were stained with hematoxylin and eosin (H&E), and the cell morphology was observed under an inverted phase contrast microscope (Olympus, Shinjuku City, Tokyo, Japan). Flow cytometry was used to identify the cell surface markers CD49d, CD90, CD105, CD34, CD45, and CD73 (Abcam, London, United Kingdom). Human adipose-derived stem cells were cultured in an adipogenic medium (Sigma) containing an high glucose-Dulbecco's modified Eagle's medium, 10% fetal bovine serum, 1 μ mol/L of dexamethasone, 10 μ mol/L of insulin, 0.5 mmol/L of 3-isobutyl-1-methylxanthine, and 200 μ mol/L of indomethacin. After 14 days of adipogenic induction, the cell morphology was observed under an inverted phase contrast microscope, and oil droplets were observed by Oil Red O staining.

The Isolation and Identification of hASC-EVs

Human adipose-derived stem cells at passage 3 to 5 were cultured until they reached 70% to 80% confluency. The medium was replaced with a serum-free Dulbecco's modified Eagle medium/Ham's F 12 nutrient medium (1:1) for 48 hours to collect a conditioned medium (100 mL total) for EV isolation. Cell debris were discarded after sequential centrifugations at 500g and 3000g for 5 and 15 minutes, respectively. The supernatant was then ultracentrifuged at 100,000g at 4°C for 1 hour, using a 45 Ti rotor (Beckman Coulter, Optimal L-80XP) and filtrated with a 0.22-mm filter (Millipore, Billerica, MA). The remaining precipitate (EVs) was resuspended in 4.0 mL of phosphate buffer saline (PBS). The EV-free medium was concentrated to 4.0 mL by ultrafiltration centrifugation via an ultrafiltration centrifuge tube (Millipore, Billerica, MA). The EV and EV-free mediums were stored at -80°C until further use. Extracellular vesicles were characterized using 80 kV transmission electron microscopy (TEM; HITACHI H-7000FA, Tokyo, Japan). The particle size distribution and concentrations of the EVs were analyzed with ZetaVIEW (ZetaVIEW S/N 17-315; Particle Metrix, Berlin, Germany) and Nanoparticle Tracking Analysis software (ZetaVIEW 8.04.02). Antibodies against TSG101, CD63, Alix, vascular endothelial growth factor (VEGF), fibroblast growth factor (FGF), and transforming growth factor β 1 (TGF β 1) (1:100; Abcam, Cambridge, United Kingdom) were used in Western blotting. In addition, the protein content of both the human adipose-derived stem cell-extracellular vesicle (hASC-EV) and EV-free medium suspensions was evaluated using a BCA Protein Assay Kit (Sigma).

Animal Model and Treatment

All animal experimental procedures were approved by the Committee of Animal Care of the Second Affiliated Hospital of Nanchang University and conducted according to the guidelines of the National Institutes of Health guide for the care and use of laboratory animals (NIH Publications Number 8023, revised 1978). Sixteen female New Zealand rabbits weighting 2.5 to 3.0 kg used in this study were obtained from the Animal Experimental Center of Nanchang University. The

rabbits were randomly divided into 2 groups (n = 8/group). The hypertrophic scar model was established as previously described.¹⁹ Briefly, the rabbits were anesthetized by an intramuscular administration of sodium pentobarbital (30 mg/kg). For each rabbit, an 8-mm-diameter wound was created down to the bare cartilage on the ventral side of both ears using an 8-mm skin punch. The epidermis, dermis, and perichondrium in each wound were thoroughly removed. After this operation, for the EV treatment group, 0.1 mL of hASC-EVs was immediately injected at the edge and base of each wound on the right ear. Meanwhile, in the same manner, 0.1 mL of PBS was injected into the left ear to form the control. For the EV-free medium treatment group, 0.1 mL of EV-free medium was immediately injected into the edge and base of each wound on the right ear, whereas 0.1 mL PBS was injected into the left ear as a control. The local injections of equal amount hASC-EV/EV-free medium and PBS were performed on postoperative day 7, 14, and 21. General views of the wounded region were photographed by digital camera on postoperative day 0, 21, and 28.

Histological Analysis

Animals were euthanized on postoperative day 28. Biopsies of the wounded skin and surrounding tissue were excised, fixed overnight in 4% paraformaldehyde and embedded in paraffin, sectioned into 5 μ m slices, and stained with H&E and Masson's trichrome. Stained sections were observed under a light microscope (Olympus, Shinjuku City, Tokyo, Japan). The maximum protuberant heights of the hypertrophic scars in each section were measured using photoshop CS6 software (Adobe, San Jose, CA). Scar elevation indexes (SEIs) were also evaluated as previously described.¹⁰

Immunofluorescence Staining

Sections were deparaffinized and incubated overnight at 4°C with mouse monoclonal to α -SMA antibody (1:50; Abcam, Cambridge, United Kingdom). The sections were placed in PBS and washed 3 times on a decolorizing shaker for 5 minutes each time. Secondary antibodies, CY3-conjugated goat antimouse (Bioss, Beijing, China), were then added for 50 minutes at room temperature in the dark. Nuclei were stained with 4',6-diamidino-2-phenylindole, and the slides were examined in a fluorescence microscope. In each section, 5 high-power fields (\times 400) on the dermis region were randomly photographed to calculate α -SMA positive cells for quantitative analysis.

Western Blotting

Tissues from both the wounded and normal skin were harvested and homogenized (12,000 g/3 minutes), and the protein was extracted with radio immunoprecipitation assay lysate. Western blot was performed to detect the protein expression of α -SMA and collagen I via the mouse monoclonal to α -SMA and collagen I antibody (1:100; Abcam, Cambridge, United Kingdom). β -Actin served as an internal normalizing standard.

Statistical Analysis

All statistical analyses were performed using GraphPad Prism software (version 7.0; GraphPad Software Inc., La Jolla, CA). Analysis of variance followed by Student *t* test was used to determine any significant differences between the 2 groups. Comparisons of multiple groups were performed with 1-way analysis of variance with corrections for multiple comparisons. Semiquantitative analysis of all the histology and cell fluorescence staining was made independently by 2 observers who were blind to the treatment conditions. *P* values of <0.05 were considered statistically significant. All values are expressed as the mean \pm SD.

RESULTS

Characterization of hASCs

Primary hASCs appeared after 5 to 7 days in culture. Under the inverted microscope, third-generation hASCs exhibited a typical

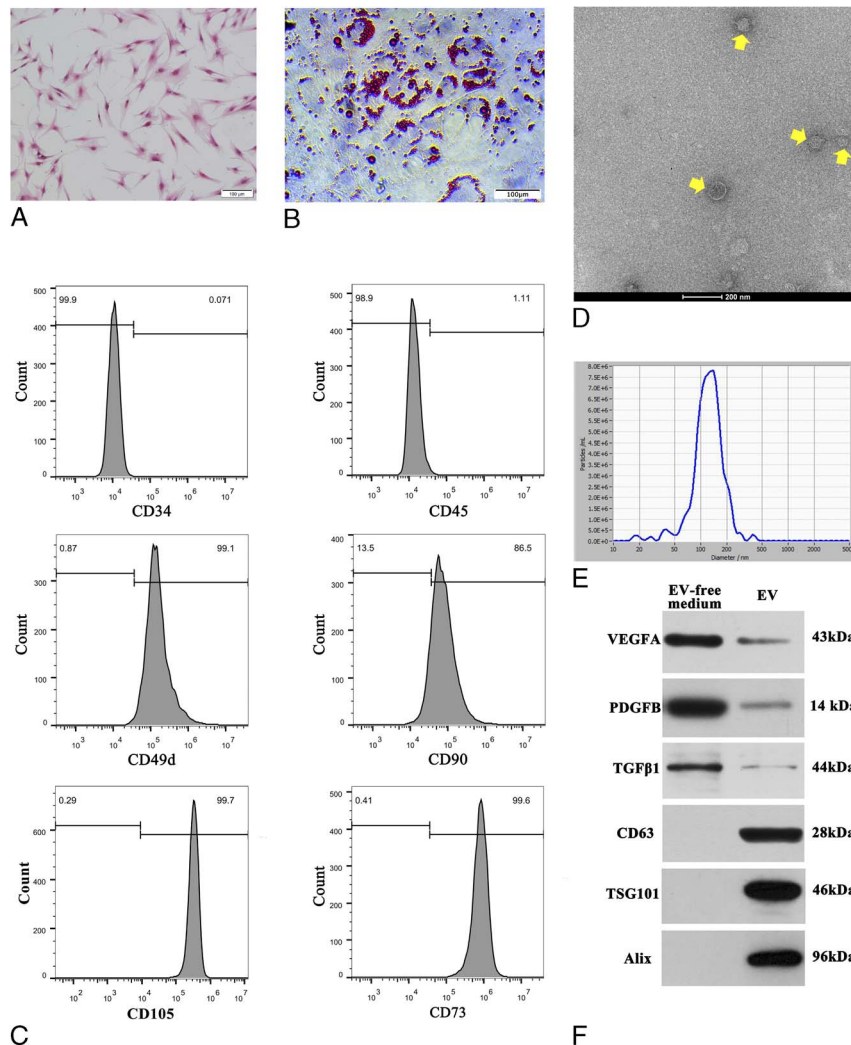


FIGURE 1. Characterization of hASCs and hASC-EVs. A, The spindle-shaped, fibroblast-like morphology of cultured (P3) hASCs. Scale bar, 100 μ m. B, Oil Red O staining for hASCs adipogenic differentiation. C, The expression of hASCs surface markers CD49d, CD34, CD45, CD90, CD105, and CD73 was measured by flow cytometry. Human adipose-derived stem cells were highly positive for CD105, CD90, CD73, and CD49d but negative for CD34 and CD45. D, The size and spheroid morphology of the hASC-EVs (pointed by yellow arrow) are shown under TEM ($\times 25,000$; 80 kV); scale bar, 200 nm. E, The particle size of the hASC-EVs was assessed by NanoSight, approximately 95% of the particles were between 50 and 200 nm in size, with an average value of 129.1 nm. F, The specific vesicle-associated markers CD63, TSG101, and Alix were mainly detected in hASC-EVs but not in the EV-free medium of hASCs by Western blot. On the contrary, vascular endothelial growth factor A, platelet derived growth factor B, and TGF β 1 were highly expressed in the EV-free medium of hASCs. [full color online](#)

fibroblastic morphology (Fig. 1A). The cells also displayed adipogenic differentiation, which was confirmed by Oil Red O staining for adipocytes (Fig. 1B). Flow cytometry analysis was performed to confirm that the hASCs expressed high levels of 49d, CD90, CD105, and CD73 and did not express CD34 or CD45 (Fig. 1C).

Characterization of hASC-EVs

The EVs extracted from the supernatant of hASCs were observed by TEM ($\times 25,000$, 80.0 kV). The majority of the hASC-EVs were circular, bilayer membrane vesicles with different sizes (Fig. 1D). NanoSight indicated that approximately 95% of the particles were between 50 and 200 nm in size, with an average value of 129.1 nm (Fig. 1E). Western blot analysis indicated that the hASC-EVs had a high expression of EV surface markers, including CD63, TSG101, and Alix but displayed a decreased expression of VEGF, FGF, and TGF β 1 when

compared with the EV-free medium (Fig. 1F). However, the EV-free medium of hASCs significantly displayed VEGF, FGF, and TGF β 1. The protein concentration of the ASC-EV suspension and EV-free medium was 45.82 μ g/mL and 126.48 μ g/mL, respectively.

hASC-EVs Suppress Hypertrophic Scar Formation in a Rabbit Scar Model

As shown in Figure 2, formatted scars treated with hASC-EVs showed a decreased height on postoperative day 28 when compared with that treated with PBS. However, there was no significant difference in scar height between the EV-free medium-treated group and the PBS group. The results of H&E, Masson's trichrome and α -SMA immunofluorescence staining revealed that the hASC-EV-treated scars showed decreased SEI (1.4 ± 0.3 vs 2.1 ± 0.4 , $n = 8$, $P < 0.05$; Figs. 3A, B), a more orderly arrangement of collagen and fewer α -SMA positive cells

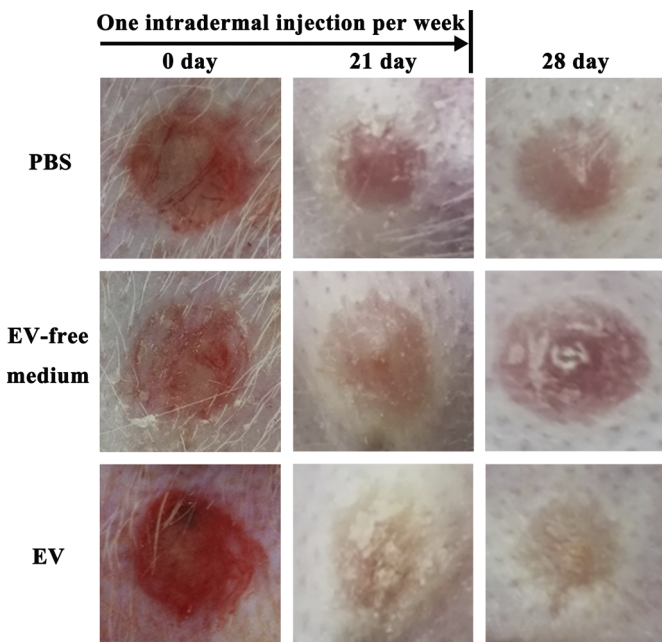


FIGURE 2. General observation of hypertrophic scars on rabbit ears. A local injection of hASC-EVs, once a week from postoperative day 0 to 21, efficiently prevented scar formation and decreased the outstanding height on postoperative day 28. [full color online](#)

(60.3 ± 23.1 vs 126.8 ± 29.9, n = 8, *P* < 0.05; Figs. 3A, C) on postoperative day 28 when compared with the PBS-treated scars. Of note, scars treated with the EV-free medium demonstrated no significant differences in the SEI, arrangement of collagen, and the count of α-SMA positive cells at postoperative day 28 when compared with that in PBS treated scars (Figs. 3A–C).

hASC-EVs Suppress Myofibroblast Formation and Collagen I Synthesis in a Rabbit Scar Model

Via Western blotting for α-SMA and collagen I, increased relative gray values of α-SMA (0.8 ± 0.2 vs 0.2 ± 0.1, n = 8, *P* < 0.05, Fig. 4A) and collagen I (1.2 ± 0.2 vs 0.9 ± 0.2, n = 8, *P* < 0.05, Fig. 4B) were detected in the scar tissue when compared with normal skin. Furthermore, hASC-EV-treated scars showed decreased relative gray values of α-SMA (0.5 ± 0.1 vs 0.8 ± 0.2, n = 8, *P* < 0.05, Fig. 4A) and collagen I (1.0 ± 0.1 vs 1.2 ± 0.2, n = 8, *P* < 0.05, Fig. 4B) when compared with PBS-treated scars. However, scars treated with an EV-free medium demonstrated no significant difference in gray values of α-SMA and collagen I as compared with PBS treated scars.

DISCUSSION

In recent years, increased evidence has indicated that the clinical application of fat grafting is of use not only for autologous aspirates but also for improving skin texture based on ASC therapies, such as wrinkles and scars.^{20,21} Several studies have reported that autologous fat/nanofat/stromal vascular fraction-gel grafting has been used for scar treatment.^{22–24} However, its biological mechanism responsible for preventing scar formation is not yet fully understood. Because few

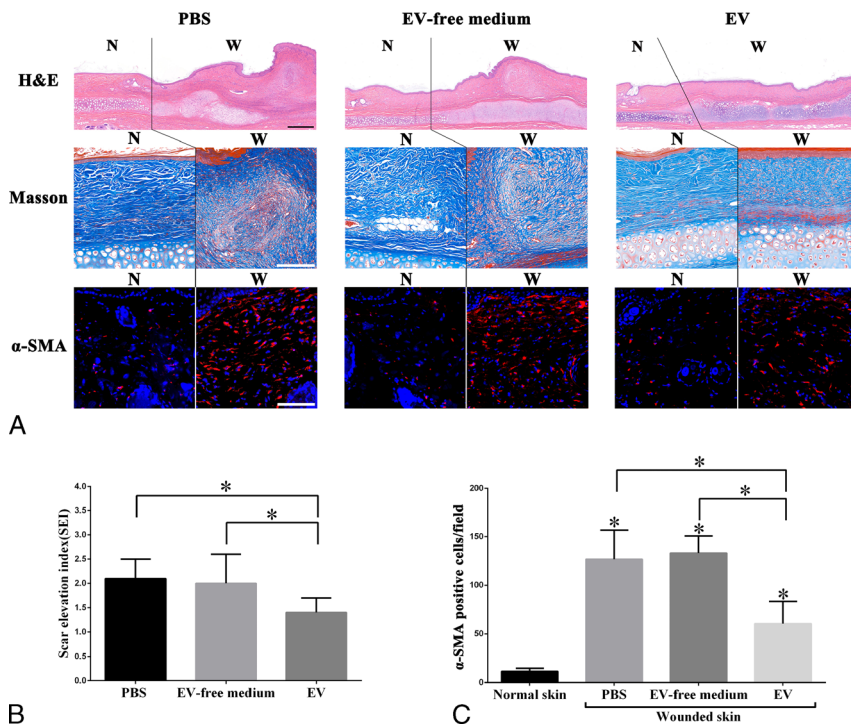


FIGURE 3. Human adipose-derived stem cell–extracellular vesicles suppress the formation of hypertrophic scars on rabbit ears. A, The results of H&E, Masson's trichrome and α-SMA immunofluorescence staining of the scars and surrounding tissues of each group at postoperative day 28. The wound area and normal skin are separated by solid lines. Treatment with hASC-EVs significantly suppressed the formation of hypertrophic scars (decreased myofibroblasts and a more orderly collagen arrangement) on rabbit ears when compared with an EV-free medium and PBS treatment; (B) Decreased scar elevation index (SEI) values were shown in wounds treated with hASC-EVs at postoperative day 28. However, few significant differences in the SEI were showed between the EV-free medium and PBS treatment. Data are presented as mean ± SD, **P* < 0.05. Scale bars in H&E staining = 500 μm, Scale bars in Masson and α-SMA immunofluorescence staining = 50 μm. [full color online](#)

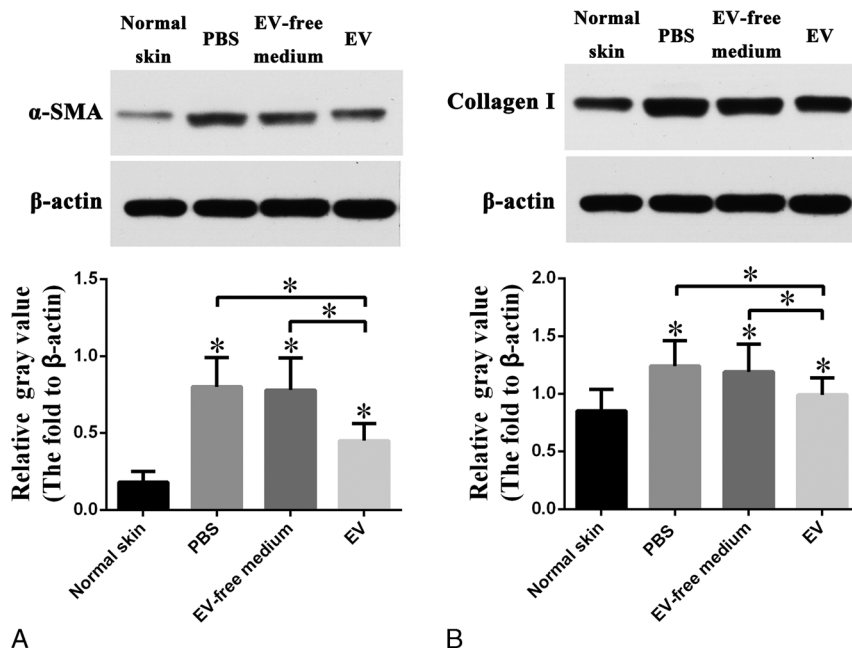


FIGURE 4. Human adipose-derived stem cell–extracellular vesicles suppress myfibroblast aggregation and collagen I synthesis after wound healing on rabbit ears. A–B, α -SMA and collagen I expression detected by Western blotting. The protein expression of α -SMA and collagen I were greatly increased in PBS treated scar tissue on postoperative day 28 when compared with normal skin, and hASC-EV treatment downregulated the expression of both α -SMA and collagen I. However, treatment with an EV-free medium of hASCs demonstrated few changes in α -SMA and collagen I expression when compared with PBS treated tissue. Data are presented as mean \pm SD, * $P < 0.05$.

mature adipocytes are content in nanofat, its function in scar prevention should be ascribed to ASCs. Zhang et al²⁵ demonstrated that local injections of ASCs inhibited the formation of hypertrophic scars in a rabbit model by decreasing α -SMA and type I collagen expression and relieving collagen deposition. Liu et al¹⁰ indicated that MSCs injected into the wounds of rabbit ears would undergo apoptosis in 12 hours. Thus, the paracrine effect of ASCs should be the major factor affecting scar formation.

Extracellular vesicles are a kind of membrane vesicles that are released from cells to the extracellular environment. They serve as a medium for intercellular signaling communication and participate in cell proliferation, apoptosis, and differentiation under physiological and pathological conditions.^{26–28} Compared with free cytokines, the inner bioactive substances of EVs, such as microRNAs and proteins, can be protected from high temperatures, various pH environments, repeated freeze-thaw cycles, and other adverse conditions by surrounding phospholipid bilayers.^{29,30} Because of a lack of immune rejection, high stability, and an easily controlled dosage and concentration, EVs have the prospect of being a nanomedicine for multiple tissue repairs.

To further clarify the main factors of an ASC-CM that benefit scar prevention, we isolated EVs and an EV-free medium from the ASC-CM and then compared the effects of both in a rabbit hypertrophic scar model. In the present study, the effects of hASC-EVs on scar prevention were significant on the postoperative day 28. Wang et al³¹ demonstrated that exosomes secreted by human adipose MSCs promoted a scarless cutaneous repair by regulating extracellular matrix remodeling. The study of Fang et al³² indicated that umbilical cord–derived MSC–derived exosomes suppressed myfibroblast differentiation by inhibiting the transforming growth factor β /Smad2 pathway during wound healing. The results of the above 2 studies on mouse models support the findings of this study. However, a rabbit ear scar model simulates a human hypertrophic scar more appropriately when compared with a mouse model.¹⁹ In addition, our results indicated that ASC-EVs were the main factor demonstrating an antiscar effect from the hASC paracrine substances, because no

significant difference was found in both gross observation and histology between the EV-free medium–treated scars and PBS-treated scars. Therefore, free cytokines, such as FGF, VEGF, and TGF β 1, enriched in an ASC-CM may promote wound healing but have no significant intervention on scar formation, especially on myfibroblast aggregation and collagen deposition, although FGF has been confirmed to inhibit scar formation.³³

Multiple clinical trials relevant to EVs, which could provide reference for future clinical trials on this therapy, have been completed. Furthermore, EVs have shown their priority in safety profile and storage compared with their parent cells.²⁸ In addition, a protocol to generate and test clinical-grade EVs has been proposed. Previous studies have revealed that the bioreactor culture of bone marrow–derived MSCs was adapted to enable the generation of large amounts of EVs from MSCs.³⁴ This provides the possibility of generating large amounts of clinical-grade EVs from ASCs. A local injection of EVs into a wound may reduce scar formation after healing, especially in wounds with high tension after routine debridement and suture, because high tension is one of the main causes of scar hyperplasia, and its application during wound healing will not prolong healing time. Thus, ASC-EVs have the prospect of being developed into a clinical antiscar drug.

There are still limitations to this study. First, ASC-EVs contain a variety of complex substances, such as proteins, RNAs, microRNAs, lincRNAs, and circRNAs, etc.^{26–28} The signaling pathway targeted by ASC-EVs in hypertrophic scar prevention, as well as the main components from the ASC-EVs involved in scar treatment, requires further study. For hypertrophic scar prevention, the optimal concentration and time point for the local injection of ASC-EVs still need to be further explored in a follow-up study.

CONCLUSIONS

The present study has clarified a new approach for hypertrophic scar prevention. A local injection of hASC-EVs during wound healing efficiently prevented hypertrophic scar formation by suppressing

myofibroblast aggregation and collagen deposition. As an alternative to cell therapy, hASC-EVs transplanted into wounds might have a clinically beneficial anticarring effect.

REFERENCES

- Han T, Lin DF, Jiang H. Wound natural healing in treatment of tumor-like hypertrophic scar. *An Bras Dermatol*. 2017;92:474–477.
- Water LV, Varney S, Tomasek JJ. Mechanoregulation of the myofibroblast in wound contraction, scarring, and fibrosis: opportunities for new therapeutic intervention. *Adv Wound Care*. 2013;2:122–141.
- Shu DY, Lovicu FJ. Myofibroblast transdifferentiation: the dark force in ocular wound healing and fibrosis. *Prog Retin Eye Res*. 2017;60:44–65.
- Shin D, Minn KW. The effect of myofibroblast on contracture of hypertrophic scar. *Plast Reconstr Surg*. 2004;113:633–640.
- Lee DE, Ayoub N, Agrawal DK. Mesenchymal stem cells and cutaneous wound healing: novel methods to increase cell delivery and therapeutic efficacy. *Stem Cell Res Ther*. 2016;7:37.
- Motegi S-I, Ishikawa O. Mesenchymal stem cells: the roles and functions in cutaneous wound healing and tumor growth. *J Dermatol Sci*. 2017;86:83–89.
- Han B, Fan J, Liu L, et al. Adipose-derived mesenchymal stem cells treatments for fibroblasts of fibrotic scar via downregulating TGF- β 1 and Notch-1 expression enhanced by photobiomodulation therapy. *Lasers Med Sci*. 2019;34:1–10.
- Fang F, Huang RL, Zheng Y, et al. Bone marrow derived mesenchymal stem cells inhibit the proliferative and profibrotic phenotype of hypertrophic scar fibroblasts and keloid fibroblasts through paracrine signaling. *J Dermatol Sci*. 2016;83:95–105.
- Du L, Lv R, Yang X, et al. Hypoxic conditioned medium of placenta-derived mesenchymal stem cells protects against scar formation. *Life Sci*. 2016;149:51–57.
- Liu S, Jiang L, Li H, et al. Mesenchymal stem cells prevent hypertrophic scar formation via inflammatory regulation when undergoing apoptosis. *J Invest Dermatol*. 2014;134:2648–2657.
- Li Y, Zhang W, Gao J, et al. Adipose tissue-derived stem cells suppress hypertrophic scar fibrosis via the p38/MAPK signaling pathway. *Stem Cell Res Ther*. 2016;7:102.
- Chen J, Li Z, Huang Z, et al. Chyle fat-derived stem cells conditioned medium inhibits hypertrophic scar fibroblast activity. *Ann Plast Surg*. 2019;83:231–277.
- Cabral J, Ryan AE, Griffin MD, et al. Extracellular vesicles as modulators of wound healing. *Adv Drug Deliv Rev*. 2018;129:394–406.
- Pelizzo G, Avanzini MA, Icaro Cornaglia A, et al. Extracellular vesicles derived from mesenchymal cells: perspective treatment for cutaneous wound healing in pediatrics. *Regen Med*. 2018;13:385–394.
- Rani S, Ritter T. The exosome — a naturally secreted nanoparticle and its application to wound healing. *Adv Mater*. 2016;28:5542–5552.
- Wang B, Li P, Shanguan L, et al. A novel bacterial cellulose membrane immobilized with human umbilical cord mesenchymal stem cells-derived exosome prevents epidural fibrosis. *Int J Nanomedicine*. 2018;13:5257–5273.
- Chen L, Brenner DA, Kisseleva T. Combatting fibrosis: exosome-based therapies in the regression of liver fibrosis. *Hepatal Commun*. 2019;3:180–192.
- Alexeev V, Arita M, Donahue A, et al. Human adipose-derived stem cell transplantation as a potential therapy for collagen VI-related congenital muscular dystrophy. *Stem Cell Res Ther*. 2014;5:21.
- Kloeters O, Tandara A, Mustoe TA. Hypertrophic scar model in the rabbit ear: a reproducible model for studying scar tissue behavior with new observations on silicone gel sheeting for scar reduction. *Wound Repair Regen*. 2007;(15 suppl 1): S40–S45.
- Wei H, Gu SX, Liang YD, et al. Nanofat-derived stem cells with platelet-rich fibrin improve facial contour remodeling and skin rejuvenation after autologous structural fat transplantation. *Oncotarget*. 2017;8:68542–68556.
- Charles-de-Sá L, Gontijo-de-Amorim NF, Maeda Takiya C, et al. Antiaging treatment of the facial skin by fat graft and adipose-derived stem cells. *Plast Reconstr Surg*. 2015;135:999–1009.
- Baptista C, Iniesta A, Nguyen P, et al. Autologous fat grafting in the surgical management of painful scar: preliminary results. *Chir Main*. 2013;32:329–334.
- Uyulmaz S, Sanchez Macedo N, Rezaeian F, et al. Nanofat grafting for scar treatment and skin quality improvement. *Aesthet Surg J*. 2018;38:421–428.
- Wang J, Liao Y, Xia J, et al. Mechanical micronization of lipospirates for the treatment of hypertrophic scars. *Stem Cell Res Ther*. 2019;10:42.
- Zhang Q, Liu LN, Yong Q, et al. Intralesional injection of adipose-derived stem cells reduces hypertrophic scarring in a rabbit ear model. *Stem Cell Res Ther*. 2015;6:145.
- Votteler J, Ogohara C, Yi S, et al. Designed proteins induce the formation of nanocage-containing extracellular vesicles. *Nature*. 2016;540:292–295.
- Nager AR, Goldstein JS, Herranz-Pérez V, et al. An actin network dispatches ciliary GPCRs into extracellular vesicles to modulate signaling. *Cell*. 2017;168:252–263.e214.
- Tkach M, Thery C. Communication by extracellular vesicles: where we are and where we need to go. *Cell*. 2016;164:1226–1232.
- Ge Q, Zhou Y, Lu J, et al. miRNA in plasma exosome is stable under different storage conditions. *Molecules*. 2014;19:1568–1575.
- Maroto R, Zhao Y, Jamaluddin M, et al. Effects of storage temperature on airway exosome integrity for diagnostic and functional analyses. *J Extracell Vesicles*. 2017;6:1359478.
- Wang L, Hu L, Zhou X, et al. Exosomes secreted by human adipose mesenchymal stem cells promote scarless cutaneous repair by regulating extracellular matrix remodelling. *Sci Rep*. 2017;7:13321.
- Fang S, Xu C, Zhang Y, et al. Umbilical cord-derived mesenchymal stem cell-derived exosomal MicroRNAs suppress myofibroblast differentiation by inhibiting the transforming growth factor- β /SMAD2 pathway during wound healing. *Stem Cells Transl Med*. 2016;5:1425–1439.
- Maddaluno L, Urwyler C, Werner S. Fibroblast growth factors: key players in regeneration and tissue repair. *Development*. 2017;144:4047–4060.
- Mendt M, Kamekar S, Sugimoto H, et al. Generation and testing of clinical-grade exosomes for pancreatic cancer. *JCI Insight*. 2018;3. pii: 99263.